Biobased Symmetrical Fatty Amides for High Heat Deflection Temperature of Poly(l -lactide)-Based Materials

Jamie Rubinstein, Etienne Grau, Patrice Dole, Guillaume Chollet, Véronique Coma, Henri Cramail

Bio-based symmetrical fatty amides for high heat deflection temperature of PLLA-based materials

AUTHOR NAMES

Jamie Rubinstein [†], Etienne Grau[†], Patrice Dole [‡], Guillaume Chollet[§], Véronique Coma[†], Henri Cramail[†*]*

AUTHOR ADDRESS

[†] LCPO/CNRS, UMR 5629, 16 Av. Pey-Berland, 33607 Pessac Cedex, France

[‡]CTCPA, Technopole Alimentec, Rue Henri de Boissieu, 01000 Bourg-en-Bresse

[§]ITERG, 11 Rue Gaspard Monge, ZA Pessac-Canéjan, 33610 Canéjan

ABSTRACT

In this paper, we report the synthesis and the use of novel fatty bis-amides as nucleating agents for PLLA to enhance its crystallisation kinetics and its heat deflection temperature using short processing times. Bis-amides were synthesised from C18 fatty acid derivatives such as stearic acid, 12-hydroxystearic acid, oleic acid or ricinoleic acid and a series of linear aliphatic diamines (C4, C6, C10 and C12), in bulk, using a thermal process. The bis-amides were then mixed with neat

PLLA through an extrusion process at different loadings (0.1wt%, 0.5wt%, 0.8wt% & 1wt%) and the resulting materials were obtained by injection-moulding. High crystallinity ratios (>50%) could be achieved through short isothermal crystallization times such as 25 seconds at 110°C and led to improved measured heat deflection temperatures nearing 120°C in the best-case scenario. Such performance was achieved using the bis-amide obtained from the C4 diamine and stearic acid, which displayed the highest melting point of all the considered nucleating agents.

KEYWORDS

Nucleating agents, PLLA, thermal resistance, bio-based fatty amides

TOC_GRAPHICAL ABSTRACT

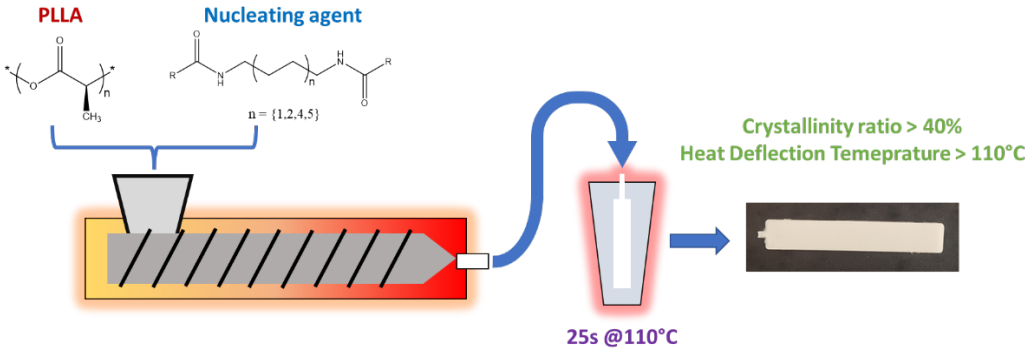

SYNOPSIS: Nucleating agents were used to enhance the heat resistance of PLLA to open new perspectives towards its use.

TEXT

INTRODUCTION

Poly(lactic acid) or poly(lactide) (PLA) is a well-known bio-based polyester, which represents a suitable alternative to oil-based non-compostable polymers. About 460,000 tons of PLA have

been produced in 2021[1] for a global market of 1.0 billion USD and therefore, the price of PLA is now nearing $2.20[2], which actually places it as an economically viable bio-based polymer material. Unfortunately, PLA carries major drawbacks to its industrial use. One of the limiting properties of PLA is its low heat deflection temperature (HDT), which is reported around 55°C[3] due to a Tg value around 55°C-60°C. Along with this, although enantiopure grades of PLA, such as poly(L-Lactide) (PLLA), can be semi-crystalline polymers, their crystallisation kinetics are too slow to get sufficiently high crystallinity ratios in fast-industrial production techniques such as the injection moulding process for instance[3–5]. This constitutes a major issue to the use of PLLA since no thermal application can be considered as such. Indeed, unless efficient means of making PLLA crystallise are developed, the fast production of crystalline PLLA materials cannot be achieved.

In this study, we focused our strategy on the use of nucleating agents (NAs) to enhance the crystallisation kinetics of PLLA directly from the melt. Many compounds have been described as successful nucleating agents, more particularly symmetric fatty amide type compounds such as N,N'-ethylene bis(stearamide) (EBS) and N-N'-ethylene bis(12-hydroxystearamide) (EBHS)[6–10] which have been reported to bring the $t_{1/2}$ of PLLA from over 30 minutes to less than 2 minutes at 1wt% loading. To our knowledge, we did not find further literature reporting the use of new C18 fatty amides as such. After further investigation, patents suggesting the efficiency of fatty amide nucleating agents with such structure were found. Takenaka *et al.* reported multiple formulations of PLLA with a glycerol-based plasticiser and a nucleating agent along with a moulding process for sheets. The maximum crystallinity ratios obtained are lower than 35% using 0.5wt% of nucleating agent and 15wt% of plasticiser. Although fatty amides obtained from fatty acids with a pendant hydroxyl group are mentioned, only EBHS and N,N'-Hexamethylenebis-12-hydroxystearic acid amide are cited as potential examples. High loadings such as 3wt% regarding

the amount of PLLA are used in this invention[11]. Onishi *et al.* later reported multiple formulations of PLLA with a glycerol fatty acid-based plasticiser and a nucleating agent along with a moulding process to obtain PLLA films with high transparency and heat resistance. This time, only 0.4wt% of nucleating agent is used with 5wt% of plasticiser and the process mentions performances achieved with the formulation directly cooled from the melt, with a moulding time of 5s. The inventors did not however specifically focussed on most C18 fatty bis-amides, with exception to EBS, EBHS, N,N'-Hexamethylenebis-12-hydroxystearic acid amide and N,N'-Xylylenebis-12-hydroxystearic acid amide[12].

Here, similar fatty bis-amide compounds were synthesised based on C18 fatty acids and a fully linear aliphatic diamine. The considered diamines have different chain lengths to change the distance between the two newly formed amide groups and to study the impact of such a change. The synthesised bis-amide compounds were then mixed to a highly optically pure PLLA to measure their effect on its crystallisation rate.

EXPERIMENTAL SECTION

*) Materials

PLLA was purchased from Natureplast (Caen, FR) under the tradename PLI 005 (D-lactide<0.5%, MFI=25-35g/min at 190°C). 1,6-diaminohexane, 1,5,7-triazabicyclo[4,4,0]dec-5-ene and stearic acid were purchased from Sigma-Aldrich. 12-hydroxstearic acid and 1,4-diaminobutane were purchased from Alfa Aesar. 1,10-diaminodecane, 1,12-diaminododecane and oleyl chloride (70%) were purchased from TCI. Methyl ricinoleate was purchased from Nu-Chek-Prep (MN, USA) with a purity over 99%. Only 1,6-diaminohexane was purified through recrystallisation in cyclohexane.

*) Nuclear Magnetic Resonance (NMR)

The ^{1}H spectra were recorded on a Bruker Advance 400 spectrometer (400 MHz for ^{1}H) by using $CDCl_3$ as a solvent at room temperature. In the case of some bis-amide compounds, a mixture of $CDCl_3$ with a few drops of hexafluoropropan-2-ol (HFIP) was used as a solvent instead. ^{1}H NMR analyses were performed with 16 scans unless mentioned otherwise.

***) Differential Scanning Calorimetry (DSC)**

Samples were analysed using a TA instruments liquid nitrogen DSC (Q100, LN2) for all DSC measurements. Samples were put through the following procedures using between 5 to 10mg: 1st heating from 20°C to 190°C, isothermal at 190°C for 10 mins, cooling at -10°C/min from 190°C to 20°C, 2nd heating at 10°C/min from 20°C to 190°C. Crystallinity ratios were measured during the first heating run through the cold-crystallisation enthalpy and the melting enthalpy using the following formula with:

$$\chi c = \frac{\Delta Hm - \Delta Hcc}{\omega PLLA * \Delta Hm, 0}$$

Equation 1. Crystallinity ratio calculation for PLLA samples

χc = the crystallinity of the PLLA sample

ΔHm = the melting enthalpy

ΔHcc = the cold-crystallisation enthalpy

$\Delta Hm,0$ = the equilibrium melting enthalpy of PLLA, 93.7 J/g[13]

$\omega PLLA$ = the weight fraction of PLLA in the sample

Melt-crystallisation points and melt-crystallisation enthalpies were measured during the cooling run. Glass transition temperatures, melting points, cold crystallisation points, melting enthalpies, and cold crystallisation enthalpies were measured during the 2nd heating run.

***) Dynamic mechanical analysis (DMA)**

DMA measurements were performed on a TA instruments Q850 DMA apparatus. Samples were run using the single cantilever oscillation mode with a heating ramp of 3°C/min from 25°C to 170°C, 1Hz, 0.1% strain with liquid nitrogen control. The Tg of the samples was measured using the onset of the storage modulus (E') curve and the Tα at the peak of the tan δ plot.

***) Polymer processing and mixing for DSC samples**

Prior to melt-blending, PLLA pellets were dried for at least 12h at 80°C in a vacuum oven. For the DSC preliminary study, the pellets and the nucleating agent were put together in a small aluminium container on hot plate set at 200°C. Once the two compounds had melted, they were stirred together using a metal spatula until the mixture looked smooth. The aluminium container was then put on the cold practice bench to cool. The total mixing time did not exceed 3 mins in order to limit the degradation of the PLLA. A small sample of about 6mg was then cut from the obtained compound to be used for DSC analysis.

***) Polymer processing and mixing for DMA samples**

Prior to melt-blending, PLLA pellets were dried at least 12h at 80°C in a vacuum oven. A Thermoscientific Minilab II HAAKE Rheomex CTW5 twin screw mini compounder with a recirculating canal was used. The temperature was set to 190°C with a rotation speed of 100 RPM (corotation mode) and a mixing time of approximately 5 mins. About 7g of compound

were loaded before being transferred to the injection moulding system. The injection moulding device is a Thermoscientific HAAKE MiniJet Pro apparatus which was heated at 183°C. The injection pressure was 400bars. A rectangular shaped mould was used to produce DMA specimens of approximately 60x10x1mm. These moulds were heated to either 63°C (cold conditions) or 110°C (hot conditions) to get either amorphous or crystallised PLLA samples.

***) Bis-amide synthesis**

C4-Stearic: 7.901g of 1,4-diaminobutane (89.6mmol) and 51g (179.3mmol) of stearic acid were put in a 500mL round bottom flask with magnetic stirring at 150°C for 24h. The obtained brown solid was ground into a powder and washed 5 times with 400mL of ethanol and left to dry under reduced pressure for 12h at 80°C to give a white slightly brown powder. Yield=92%.

C6-Stearic: 5.106g of 1,6- diaminohexane (43.94mmol) and 25g (87.88mmol) of stearic acid were put in a 250mL round bottom flask with magnetic stirring at 150°C for 24h. The obtained brown solid was ground into a powder and washed 3 times with 400mL of ethanol and left to dry under reduced pressure for 12h at 80°C. Yield=88%.

C10-Stearic: 302.94mg of 1,10-diaminodecane (1.758mmol) and 1g (3.515mmol) of stearic acid were put in a 25mL round bottom flask with magnetic stirring at 150°C for 6h under vacuum. The obtained brown solid was ground into a powder and washed 3 times with 20mL of tetrahydrofuran and left to dry under reduced pressure for 12h at 80°C to give a white slightly brown powder. Yield=69%.

C12-Stearic: 352.15mg of 1,12-diaminododecane (3.515mmol) and 1g (1.758mmol) of stearic acid were put in a 500mL round bottom flask with magnetic stirring at 150°C for 6h under

vacuum. The obtained brown solid was ground into a powder and washed 3 times with 20mL of tetrahydrofuran and left to dry under reduced pressure for 12h at 80°C to give a white slightly brown powder. Yield=53%.

C4-12-HSA: 2.567g of 1,4-diaminobutane (29.12mmol) and 17.5g (58.24mmol) of 12-hydroxystearic acid were put in a 100mL round bottom flask with magnetic stirring at 150°C for 24h. The obtained brown solid was ground into a powder and washed 5 times with 200mL of ethanol and left to dry under reduced pressure for 12h at 80°C to give a white slightly brown powder. Yield=75%.

C6-12-HSA: 3.38g of 1,6-diaminohexane (29.12mmol) and 17.5g (58.24mmol) of 12-hydroxystearic acid were put in a 100mL round bottom flask with magnetic stirring at 150°C for 24h. The obtained brown solid was ground into a powder and washed 3 times with 200mL of ethanol and left to dry under reduced pressure for 12h at 80°C to give a white slightly brown powder. Yield=77%.

C10-12-HSA: 286.7mg of 1,10-diaminodecane (1.664mmol) and 1g (3.328mmol) of 12-hydroxystearic acid were put in a 25mL round bottom flask with magnetic stirring at 150°C for 24h under vacuum. The obtained brown solid was ground into a powder and washed 3 times with 20mL of ethanol and twice with 20mL of tetrahydrofuran and left to dry under reduced pressure for 12h at 80°C to give a white slightly brown powder. Yield=59%.

C12-12-HSA: 333.4mg of 1,12-diaminododecane (1.664mmol) and 1g (3.328mmol) of 12-hydroxystearic acid were put in a 25mL round bottom flask with magnetic stirring at 150°C for 31h under vacuum. The obtained brown solid was ground into a powder and washed 3 times with

20mL of ethanol and twice with 20mL of tetrahydrofuran and left to dry under reduced pressure for 12h at 80°C to give a white slightly brown powder. Yield=65%.

C4-Oleic: 146.5mg of 1,4-diaminobutane (1.66mmol) were put in 10mL of dichloromethane upon which 10mL of an aqueous solution of NaOH(aq) at 1mol/L were added under low stirring. 1.176g (3.35mmol) of oleyl chloride (85% pure) were slowly added using a syringe directly into the organic phase at room temperature and left for 2h. The obtained white powder was washed with dichloromethane, water and diethyl ether and left to dry under reduced pressure for 12h at 80°C. Yield=32%.

C6-Oleic: 193.1mg of 1,6-diaminohexane (1.66mmol) were put in 10mL of dichloromethane upon which 10mL of an aqueous solution of NaOH(aq) at 1mol/L were added under low stirring. 1.176g (3.35mmol) of oleyl chloride (85% pure) were slowly added using a syringe directly into the organic phase at room temperature at left for 2h. The obtained white powder was washed with dichloromethane, water and diethyl ether and left to dry under reduced pressure for 12h at 80°C. Yield=37%.

C10-Oleic: 286.3mg of 1,10-diaminodecane (1.66mmol) were put in 10mL of dichloromethane upon which 10mL of an aqueous solution of NaOH(aq) at 1mol/L were added under low stirring. 1.176g (3.35mmol) of oleyl chloride (85% pure) were slowly added using a syringe directly into the organic phase at room temperature at left for 2h. The obtained white powder was washed with dichloromethane, water and diethyl ether and left to dry under reduced pressure for 12h at 80°C. Yield=67%.

C12-Oleic: 332.9mg of 1,12-diaminododecane (1.66mmol) were put in 10mL of dichloromethane upon which 10mL of an aqueous solution of NaOH(aq) at 1mol/L were added

under low stirring. 1.176g (3.35mmol) of oleyl chloride (85% pure) were slowly added using a syringe directly into the organic phase at room temperature at left for 2h. The obtained white powder was washed with dichloromethane, water and diethyl ether and left to dry under reduced pressure for 12h at 80°C. Yield=66%.

C4-Ricinoleic: 500 mg of methyl ricinoleate, 93.0mg of 1,4-diaminobutane and 44.6mg of TBD (1:0.5:0.2, molar ratios) were put in a Schlenk tube with a condenser and a magnetic stirrer at 120°C for 3h then under vacuum for 1h at 120°C. The white solid was recuperated and washed with 50mL of water and 15mL of cold ethanol. Yield=30%.

C6-Ricinoleic: 1g of methyl ricinoleate, 185.9mg of 1,6-diaminohexane and 89.1mg of TBD (1:0.5:0.2, molar ratios) were put in a Schlenk tube with a condenser and a magnetic stirrer at 120°C for 3h then under vacuum for 1h at 120°C. The solid was recuperated and washed with 50mL of water and 15mL of cold ethanol. Yield=25%.

C10-Ricinoleic: 1g of methyl ricinoleate, 275.3mg of 1,10-diaminodecane and 89.1mg of TBD (1:0.5:0.2, molar ratios) were put in a Schlenk tube with a condenser and a magnetic stirrer at 120°C for 3h then under vacuum for 1h at 120°C. The solid was recuperated and washed with 15mL of cold ethanol. Yield=29%.

C12-Ricinoleic: 1g of methyl ricinoleate, 320.6mg of 1,12-diaminododecane and 89.1 mg of TBD (1:0.5:0.2, molar ratios) were put in a Schlenk tube with a condenser and a magnetic stirrer at 120°C for 3h then under vacuum for 1h at 120°C. The solid was recuperated and washed with 15mL of cold ethanol. Yield=35%.

RESULTS AND DISCUSSION

Bis-amide structure

Sixteen different bis-amides were synthesised using the protocols described above. The concept was similar: a fatty acid derivative was put to react with a linear aliphatic diamine to yield a symmetric bis-amide compound. Four C18 fatty acids or their derivatives were used: stearic acid, 12-hydroxystearic acid, oleic acid and ricinoleic acid. Regarding the diamines, four different linear aliphatic diamines were used containing either four, six, ten or twelve methylene groups between the two amine groups. The idea is to study the effect of the chain spacer between the formed amide functions on the properties of the synthesized compounds (structure in **Figure 1**).

Figure 1

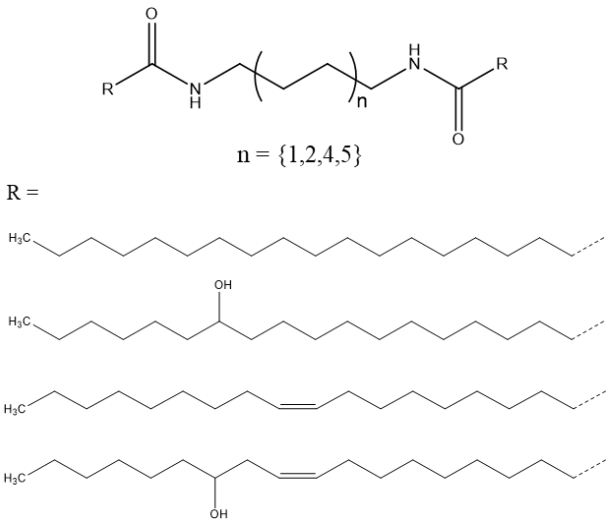

Figure 1. Structure of the synthesised bis-amide compounds

The structure and the purity of the synthesised compounds was confirmed by ^{1}H NMR (**Supporting Information**, Figure S1 to Figure S4) with a triplet appearing at 3.2-3.3 ppm accounting for the two protons in alpha of the formed amide groups and a signal appearing at 5.8-

6.0 ppm accounting for the labile proton of the formed amide group. The integration of the signal at 6.0 ppm gave the purity of the synthesised compounds which are summarized in Table 1.

Bis-amide properties

The melting point and the crystallisation point of the synthesised products were then measured by means of the DSC. The thermograms corresponding to the stearic acid-based show very well-defined melting endotherms and crystallisation exotherms. For the 12-hydroxystearic acid derivatives, the C10-12-HSA and to some little extent the C6-12-HSA bis-amides seem to display overlapping melting peaks. This was attributed to the polymorphism of crystalline fatty derivatives which was reported in different studies ([14–16]). In the case of the oleic acid-based compounds, small second endotherms and exotherms could also be seen. The NMR spectra do not show any residual free amine, therefore the origin of these peaks was attributed to the polymorphism of the compounds due to the configuration of the fatty chain ([16]). In the case of the ricinoleic-based bis-amides, broader melting peaks and crystallisation peaks were observed in the case of C4-Ric and C6-Ric, due to the lower purity and the presence of TBD or mono-amide (DSC traces in **Supporting Information**, Figure S5 and Figure S6).

Looking at the trend, the highest melting points are obtained for the stearic derived compounds, which corresponds to a fully aliphatic fatty C18 chain. The second most high melting points are obtained for the 12-hydroxystearic derived bis-amides then the oleic derivatives and finally the ricinoleic one. It is possible to notice the effect of the fatty chain on the melting point of the bis-amides: a fully aliphatic and linear chain will provide the highest melting points whereas a substituted chain with a hydroxyl group and an unsaturation will lead to lower melting point values. This is in accordance with common knowledge relating to intermolecular interactions. The

presence of an unsaturation will lead to less favourable packing of the molecules between themselves due to an effect on the chain configuration. This can also be true in the case of the presence of a hydroxyl group which might partially block the trans-trans configuration of the chains. Therefore, less energy will be required to break such assembly leading to lower melting points than in the case of the fully linear and aliphatic carbon chain.

Table 1

Fatty acid	Diamine	$Purity_{NMR}$ (%)[a]	$Purity_{SEC}$ (%)[b]	ΔH_m (kJ/mol)[c]	T_m (°C)[c]	T_c (°C)[d]
Stearic	C4	94	-	117.3	150	146
	C6	98	-	127.2	145	141
	C10	95	-	134.2	140	134
	C12	97	-	146.5	138	133
12-hydroxystearic	C4	93	-	84.2	142	137
	C6	96	-	89.4	136	130
	C10	95	-	113.4	131	125
	C12	95	-	149.6	139	136
Oleic	C4	98	-	62.0	110	105
	C6	98	-	72.5	109	103
	C10	98	-	94.6	109	102
	C12	97	-	105.3	109	103
Ricinoleic	C4	93	94	59.4	93	79
	C6	82	88	64.4	88	60
	C10	95	99	87.5	102	90
	C12	94	95	95.9	103	91

Table 1: Degree of purity and thermal characteristics of the synthesised bis-amides a) ^{1}H NMR, $CDCl_3$, 400MHz, b) SEC in THF vs PS, 40°C, 1mL/min, c) DSC 2nd heating 20°C to 190°C, 10°C/min, d) DSC cooling 190°C to 20°C, -10°C/min

Looking at the different amines used, namely the different chain spacers between the two amide groups, a trend for the stearic derivatives can be noticed showing that the longer the chain of the diamine, the lower the melting point. This was mainly attributed to the decreasing amide group content in the molecular chain, that is to say, a lower hydrogen-bond density due to the increase of the number of methylene groups with longer diamines. As also reported by Stempfle *et al.* ([17]), van der Waals interactions between hydrocarbon segments only contribute to a minor role. This behaviour and melting point values have been also reported by Poopalam *et al.* ([16]). As per a similar trend with non-fully aliphatic bis-amides, the DSC revealed nothing as such. In the case of the 12-hydroxystearic derivatives, the trend was verified for C4-12-HSA, C6-12-HSA, and C10-12-HSA but the melting point of C12-12-HSA was higher than the one of C12-12-HSA. This can be explained by a more predominant effect of the hydrocarbon chains' intermolecular interactions between each other on the crystallisation process rather than the H-bonding effect between the amide groups. For all oleic derivatives, the melting point was rather similar and around 110°C. Finally, in the case of the ricinoleic based bis-amides, the trend was completely opposite, the longer the diamine chain, the higher the melting point. However, this to be further examined and discussed. Indeed, highly pure compounds could be due to difficulties during the purification step. Therefore, the low melting point and crystallisation point of C6-Ric could be explained by the presence of remaining TBD. For C4-Ric, an effect might be measured through the presence of 10 to 14% of mono-amide, as revealed by NMR and SEC, with a lower melting point.

Preliminary DSC study

The results reported from the DSC analysis allow us to pre-determine the best nucleating agents from the ones synthesised. Neat PLLA has very slow crystallisation kinetics, only a crystallinity

ratio below 10% in controlled cooling conditions. Crystallinity ratios over 50% could be obtained with bis-amides based on stearic acid and 12-hydroxystearic acid in the same controlled cooling conditions. More precisely, such performance was achieved using the shorter diamines which are the C4-diamine and the C6-diamine. When the C10-diamine and the C12-diamine were used, there was also an enhancement in the crystallinity ratio, however, it was at least 20% lower than the ones previously described. Comparatively, the crystallinity ratios obtained using nucleating agents synthesised from either the oleic acid derivative or the ricinoleic acid one stayed below 25% therefore making these group of bis-amides the less efficient in these dynamic cooling conditions.

Table 2

Fatty acid	Diamine	ΔH_c (J/g)[a]	ΔH_{cc} (J/g)[b]	ΔH_m (J/g)[b]	$\Delta H_{\alpha' \rightarrow \alpha}$ (J/g)[b]	$\chi_{c,m}$ (%)[a]	$\chi_{c,c}$ (%)[b]	T_g (°C)[b]	T_c (°C)[a]	T_m (°C)[b]
PLA	-	5.34	40.5	49.2	0.59	**6**	**9**	60	111	173
Stearic	C4	45.1	-	49.1	-	**48**	**52**	62	120	173
	C6	43.3	-	49.9	-	**46**	**53**	62	115	172
	C10	20.9	18.1	55.1	3.13	**22**	**36**	60	113	172
	C12	16.3	21.8	55.2	2.93	**17**	**33**	59	114	172
12-hydroxystearic	C4	37.9	3.14	52.4	1.56	**41**	**51**	59	113	172
	C6	44.5	-	55.9	-	**48**	**60**	62	113	173
	C10	12.7	24.9	53.8	4.10	**14**	**27**	60	113	172
	C12	12.9	23.0	51.6	3.62	**14**	**27**	60	114	172
Oleic	C4	14.7	26.4	52.5	3.57	**16**	**24**	59	112	171
	C6	9.84	30.2	52.5	5.44	**11**	**18**	60	112	172
	C10	12.2	28.4	53.7	4.96	**13**	**22**	60	112	172
	C12	13.6	27.0	54.1	5.43	**15**	**23**	60	112	172
Ricinoleic	C4	9.17	36.2	55.4	3.50	**10**	**17**	59	115	171
	C6	3.59	45.8	52.4	2.63	**4**	**4**	58	110	168
	C10	8.98	38.9	56.7	3.50	**10**	**15**	59	114	172
	C12	7.27	40.6	54.7	3.54	**8**	**11**	59	112	171

Table 2: DSC results of preliminary samples of PLLA + 1wt% of synthesised fatty NA

Looking at these performances in regard of the respective melting points and crystallisation points of the bis-amides, a clear effect of the thermal transitions on the nucleation efficiency can be seen. The most efficient nucleating agents have melting points and crystallisation points above 130°C, which corresponds to the upper limit of the temperature window in which PLLA can crystallise. Indeed, neat PLLA is reported to only be able to crystallise between 80°C and 130°C ([4,18,19]). Here, the best nucleating agents all crystallise before PLLA starts crystallising or just as it would as observed by Nam *et al.* with EBHS ([6]). This also explains why other nucleating agents from oleic acid derivatives or ricinoleic acid derivatives, all with crystallisation points in the low temperature range of crystallisation of PLLA, are not as efficient as the ones made from stearic acid and 12-hydroxystearic acid. In effect, we suggest that fully crystallised nucleating agents have created multiple nuclei in the PLLA matrix therefore greatly enhancing the crystallisation kinetics by partially getting rid of the energy barrier required for nucleation during the crystallisation process of PLLA. Therefore, nucleating agents with the highest melting points and crystallisation points seem to be more efficient. Moreover, if the compounds' dispersion in PLLA is good, this would allow a very homogeneous nucleation and therefore limit the amount of time needed for crystalline growth since most of the PLLA matrix would start crystallising at the same time.

However, just a difference in melting points and crystallisation points might not be sufficient as an explanation. In the case of 12-HSA derived bis-amides, a higher crystallisation point for the C12-bis-amide than for the C6-bis-amide was reported, although the C6-bis-amide remains the more efficient of the two. Intermolecular interactions could be at play here since there is a 6-carbon atom difference in space between the amide functions of these two molecules. It therefore seems that closer amide functions would create more favourable interactions with the PLLA matrix to promote the crystallisation phenomenon. This would also be in accordance with polarised optical

microscopy reported by Nam *et al.* ([6]) in which they noticed an epitaxial growth of oriented PLLA crystals at the interface between the crystallised nucleating agent and the PLLA melt. Far from this interface, the PLLA would crystallise in its regular spherulite morphology.

Melt-blending to make DMA samples in isothermal conditions

*) Preliminary study: mould temperature screening

Thanks to the preliminary DSC analysis, the focus was put on evaluating the efficiency of two specific families of the selected bis-amides which are the bis-amides obtained from stearic acid and the ones obtained from 12-hydroxystearic acid. Indeed, the highest crystallisation enthalpies upon cooling from the melt were measured with these two groups of nucleating agents and accordingly, the highest crystallinity ratios. To go further in this study, the nucleating agents were blended in PLLA using a twin-screw mini extruder with a recirculating canal to properly mix the compounds and to use the injection moulding technique to produce DMA samples. These DMA samples would be used to test different isothermal moulding conditions and evaluate the performance of our nucleating agents in such isothermal conditions. Three different isothermal moulding temperatures were tested first: 95°C, 100°C and 110°C for PLLA samples with a 1wt% of nucleating agent and held the sample inside the mould for 75s. Afterwards, a moulding temperature of 110°C was chosen, the amount of nucleating agent was diminished, and also the moulding time was reduced from 75s to 25s which is the fastest time that can be reproducibly obtained using our apparatus. The idea here was to gather finer information about the performance of the nucleating agents, how low could we go in terms of composition and how fast the injection moulding process could be to have highly crystallised PLLA samples in favourable temperature conditions. Typical obtained samples are shown in Figure 2.

Figure 2

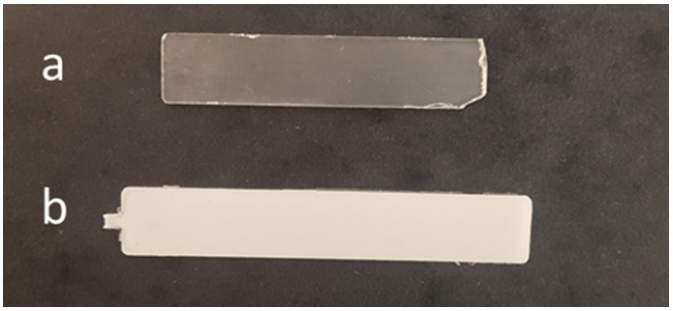

Figure 2. DMA samples of an injection moulded a) neat PLLA, b) PLLA + 1wt% Stear-C4 at 110°C for 75secs

The obtained samples were analysed by means of the DSC and dynamic mechanical analysis (DMA). The DSC analysis was used to measure the crystallinity ratio of the samples whereas the DMA was used to evaluate the thermo-mechanical behaviour of the considered samples as the latter gives a very good picture of the low HDT of PLLA. As shown in Figure 3, highly amorphous PLLA will display a huge drop of storage modulus (E') just after the temperature reaches 55-60°C. This is typical since the crystallisation kinetics of PLLA are very slow, it will not be able to crystallise during fast means of production such as injection moulding in a cold mould. Therefore, as the temperature goes above the Tg of PLLA, there will not be any crystalline segments holding the PLLA chains, which are able to move between one another at such temperature. This leads to the observed fall of the storage modulus by more than a hundred-fold and the very high peak on tan δ. The increase later observed corresponds to the cold crystallisation of PLLA, starting around 80°C, which can be verified using the DSC as shown in Figure 4. The second sample represented in Figure 3 is also PLLA but injection-moulded at 110°C for 75secs which will be the reference time for preliminary testing of the selected nucleating agents. Here, the drop of modulus is not as

strong as for the quenched amorphous sample thanks to a higher crystallinity ratio as shown in the data collected in

Table 3.

Figure 3

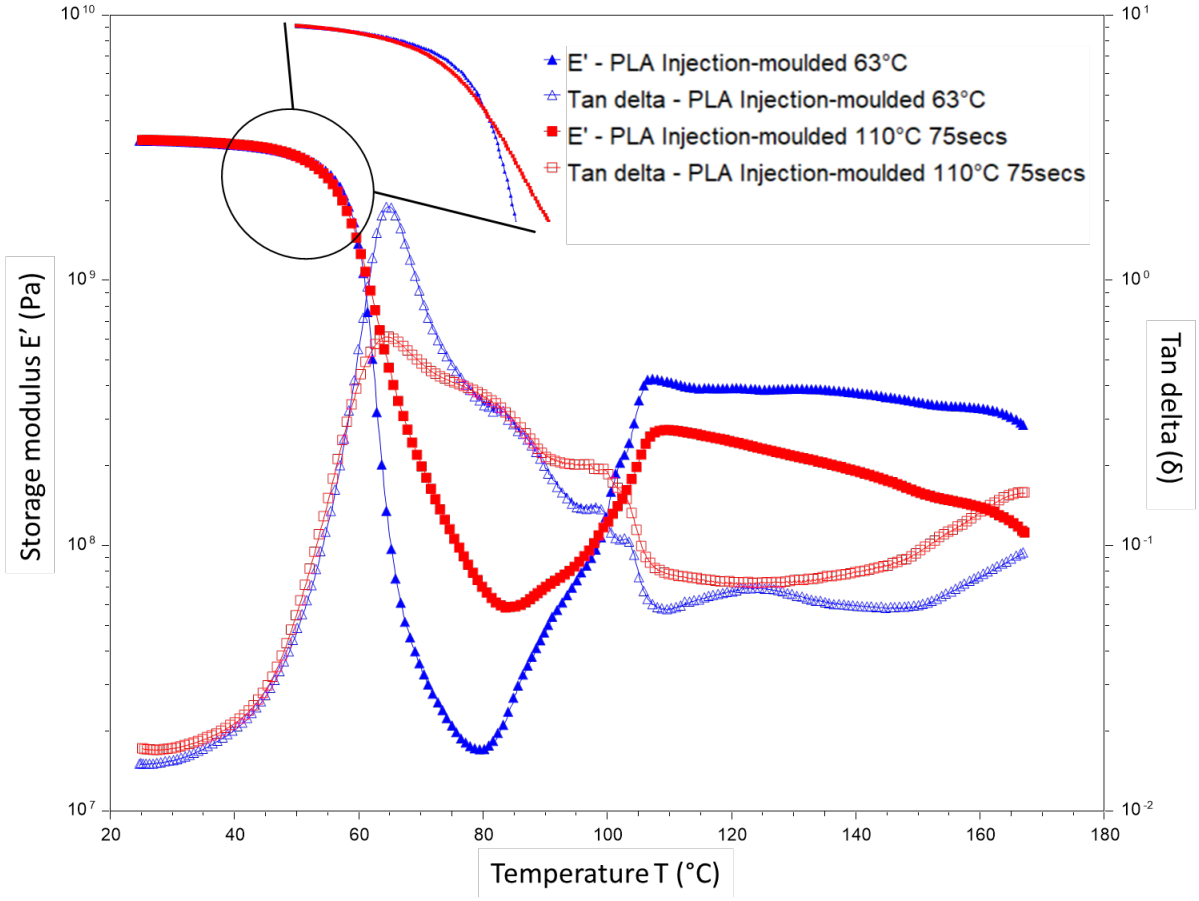

Figure 3. Storage modulus (full symbols) and tan δ (empty symbols) vs temperature (heating 3°C/min) of neat PLLA injection moulded at 63°C (quenched - triangles) and 110°C for 1min 15s (hot - squares)

Table 3

Sample	Mould temperature (°C)	Onset E' (°C)[a]	Max tan δ (°C)[a]	HDT (°C)[a]	$\chi_{c,c}$ (%)[b]	T_g (°C)[b]	T_m (°C)[b]
Neat PLA	63	59.6	64.9	63	**4**	57	174
	110	56.7	64.5	67	**15**	54	174

Table 3. DMA and DSC data for neat PLLA moulded at 63°C and 110°C

Figure 4

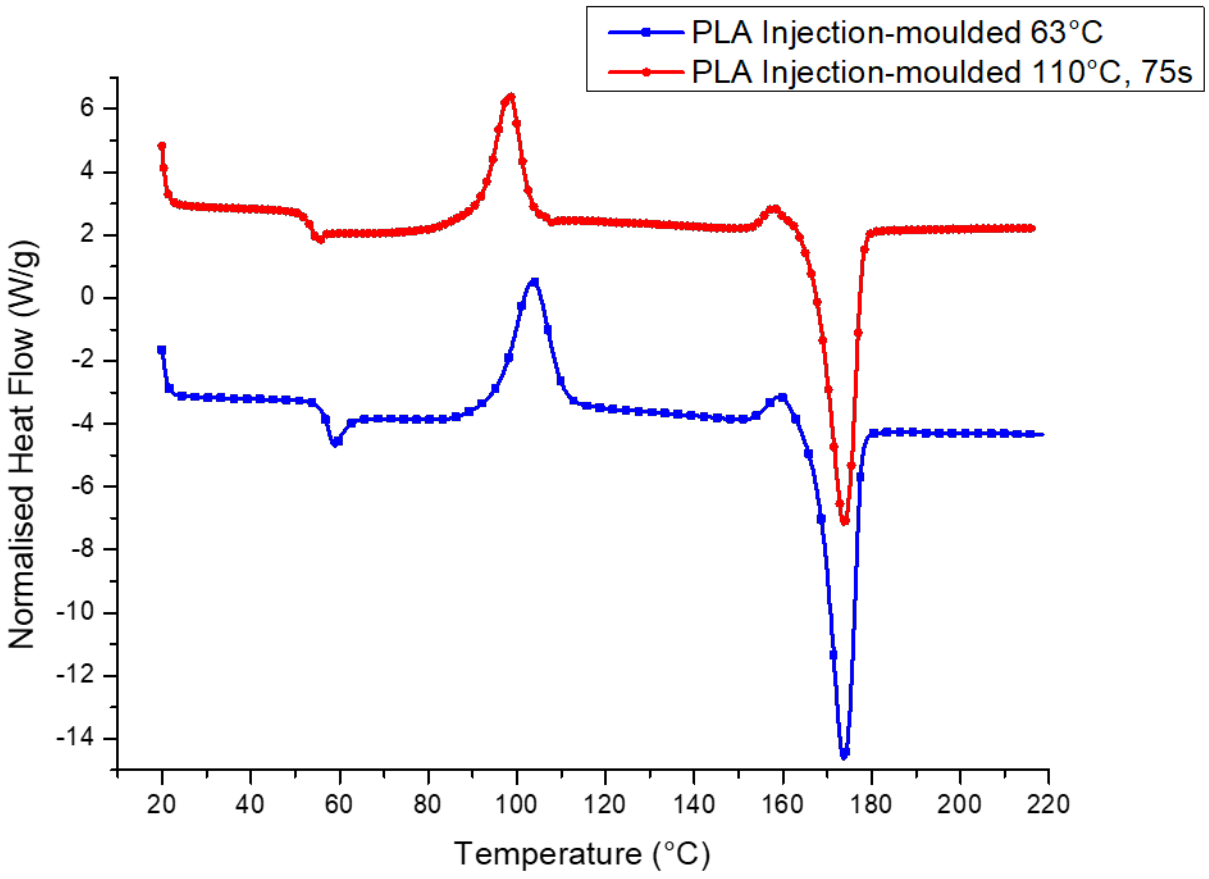

Figure 4. DSC traces of PLLA injection moulded at 63°C and 110°C for 1min 15s, 1st heating, 10°C/min

The heat deflection temperature (HDT) was measured by taking the temperature at which the storage modulus value is equal to a tenth of its value at 25°C. Surprisingly, the onset temperature

for the decrease of E' at the Tg is higher for the quenched PLLA with the lower crystallinity ratio. We would have predicted the opposite since a higher onset temperature usually is proof of an increased thermal resistance. We also did not expect to find the maximum of tan δ at the same temperature as we would have assumed a higher temperature for the more crystallised sample. However, when looking at the HDT criterion, a small increase from 63°C to 67°C could be noticed, which does not represent a real difference in terms of heat resistance. All in all, a 10% crystallinity ratio is insufficient to make a real difference for PLLA in terms of thermal resistance and properties.

Figure 4 gives us also an idea of the difference in thermal behaviour of the two samples. First of all, the cold crystallisation peaks differ since the one for the 110°C injection-moulded sample is narrower and starts at lower temperatures than the one for the 63°C injection-moulded PLLA. Moreover, there is also a small exotherm present just before the melt endotherm in the 110°C moulded sample. This is known to be a solid-state transition from the α' form to the more stable α form of PLLA prior to melting. This would suggest that our moulding process will favour the creation of the α' crystalline form of PLLA. This has been confirmed further by means of XRD for the tested samples (see **Supporting Information** Figure S7 and Figure S8).

At first, to test the efficiency of our nucleating agents, the composition was set to 99 parts of PLLA and 1 part of NA per weight. The moulding time was set to 1min 15s and only the mould temperature was changed. The samples were analysed through the DSC and the DMA, and the results are reported in Table **4**.

Table 4

Fatty acid	Diamine	Temperature (°C)	Onset E' (°C) [a]	Max tan δ (°C) [a]	HDT (°C)[a]	$\chi_{c,c}$ (%)[b]	T_g (°C)[b]	T_m (°C)[b]
Stearic	C4	95	57.9	73.0	**96**	**48**	51	173
		100	58.1	73.8	**102**	**48**	51	172
		110	58.3	73.2	**119**	**57**	57	174
	C6	95	56.7	73.4	**93**	**48**	56	173
		100	57.2	72.5	**103**	**47**	51	173
		110	58.5	73.3	**115**	**58**	53	173
	C10	95	57.2	64.8	**66**	**19**	56	173
		100	58.1	67.2	**78**	**35**	55	172
		110	57.3	71.0	**102**	**47**	54	173
	C12	95	56.6	63.7	**63**	**21**	55	172
		100	57.7	65.9	**73**	**24**	61	173
		110	57.4	70.1	**81**	**34**	53	173
12-hydroxystearic	C4	95	58.0	65.6	**65**	**20**	55	172
		100	56.8	66.4	**72**	**35**	55	173
		110	58.7	73.5	**107**	**51**	53	174
	C6	95	56.3	64.3	**66**	**28**	53	173
		100	56.0	69.9	**81**	**34**	54	173
		110	57.4	72.7	**105**	**51**	54	174
	C10	95	56.7	63.4	**63**	**20**	55	172
		100	56.7	64.9	**68**	**23**	55	166
		110	56.8	66.0	**73**	**28**	55	173
	C12	95	57.1	63.5	**63**	**27**	56	173
		100	57.3	64.2	**67**	**28**	56	173
		110	56.0	68.8	**79**	**47**	52	173

Table 4. Thermal and thermo-mechanical analysis of injection moulded samples in different isothermal conditions, a) DMA from 25°C to 170°C, 1Hz, 0.1% strain b) DSC 1st heating 20°C to 190°C,10°C/min

The first observation that can be made is that the best moulding temperature is 110°C. Indeed, whatever the considered formulation, the highest crystallinity ratios were always measured when the sample had been made at 110°C. Along with the crystallinity ratio, the highest HDTs are obtained using the mould at that temperature for the different samples. Jointly, the best performances in terms of crystallinity ratio were obtained with the shorter diamines (C4 and C6), as expected from the DSC preliminary results. This is further confirmed by samples with high crystallinity ratios giving high HDTs, which is consistent with the behaviour of a semi-crystalline

polymer. The HDT is improved from 63°C for an amorphous PLLA to 119°C in the best-case scenario (1wt% C4-Stear at 110°C), closely followed by the sample with 1wt% C6-Stear at 110°C, both samples respectively having crystallinity ratios of 57% and 58%. The trend with the other samples was expected: the lower the crystallinity ratio, the lower the HDT.

The importance of the melting point and crystallisation temperature of the nucleating agents was also shown. Globally, for the same fatty acid precursor of a bis-amide, the lower the crystallisation temperature, the less efficient it will be regarding the nucleation phenomenon. This is particularly verified in the case of the 12-hydroxystearic acid derivatives where the C12-12-HSA bis-amide exhibited a higher crystallisation point (136°C) than the C10-12-HSA bis-amide (125°C) and consequently gave samples with higher crystallinity ratios. Regarding the performance achieved by neat PLLA, the onset temperatures for the storage moduli were slightly higher when high crystallinity ratios were achieved, around 59°C-60°C. More importantly, the temperature corresponding to the maximum value of the tan δ curve shifted more significantly, now reaching values above 70°C compared to 65°C previously measured. Also, a slight shift of the Tg could be measured towards higher values in some cases but was not consistent with the measured crystallinity ratios due to the bad thermal contact of the sample in the DSC pan.

Two DMA plots from Figure 5 illustrate the performance of the 8 nucleating agents on the storage modulus of the samples versus the temperature. It is interesting to notice the effect of the crystallinity ratios on the thermo-mechanical behaviour of the samples at temperatures higher than the Tg of PLLA. Compared to the PLLA reference also moulded at 110°C, the fall of modulus is indeed being reduced thanks the crystalline zones within our PLLA samples. Another noticeable behaviour is the higher the crystallinity ratio, the less the drop of the storage modulus. In the case

of samples reaching over 50% crystallinity ratios, there was no pit shaped fall of storage modulus, accounting for a much better thermal resistance behaviour.

Figure 5

a) Effect of stearic bisamide derivatives on PLLA

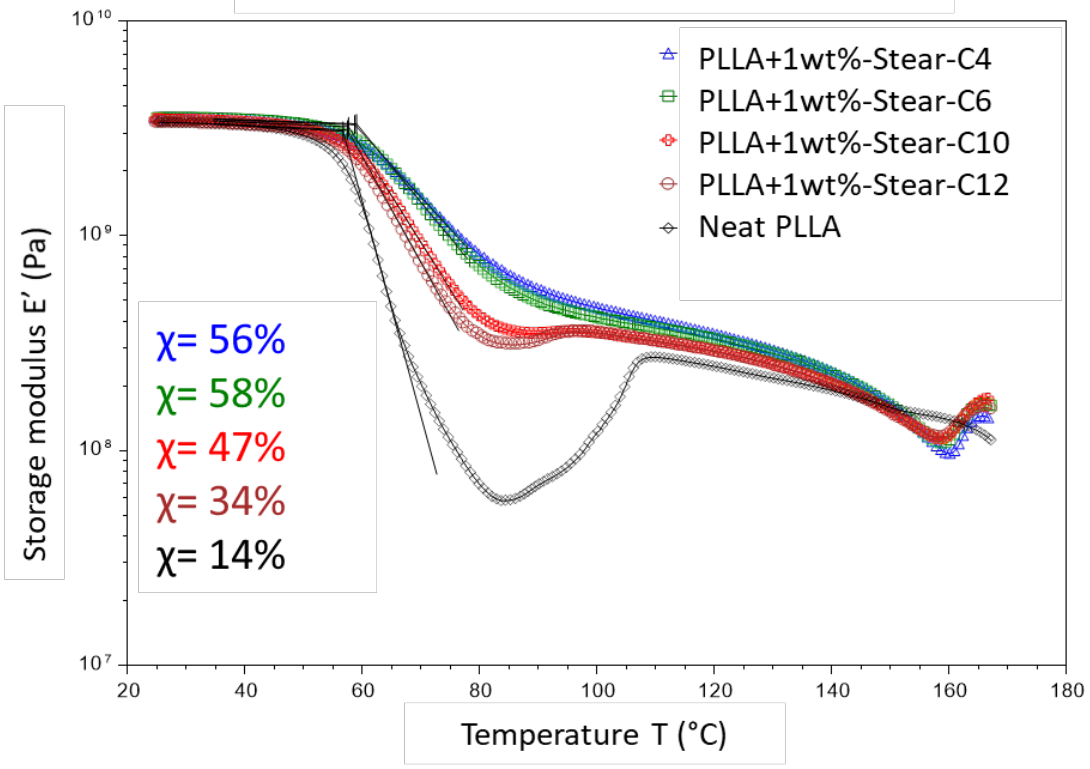

b) Effect of 12-HSA bisamide derivatives on PLLA

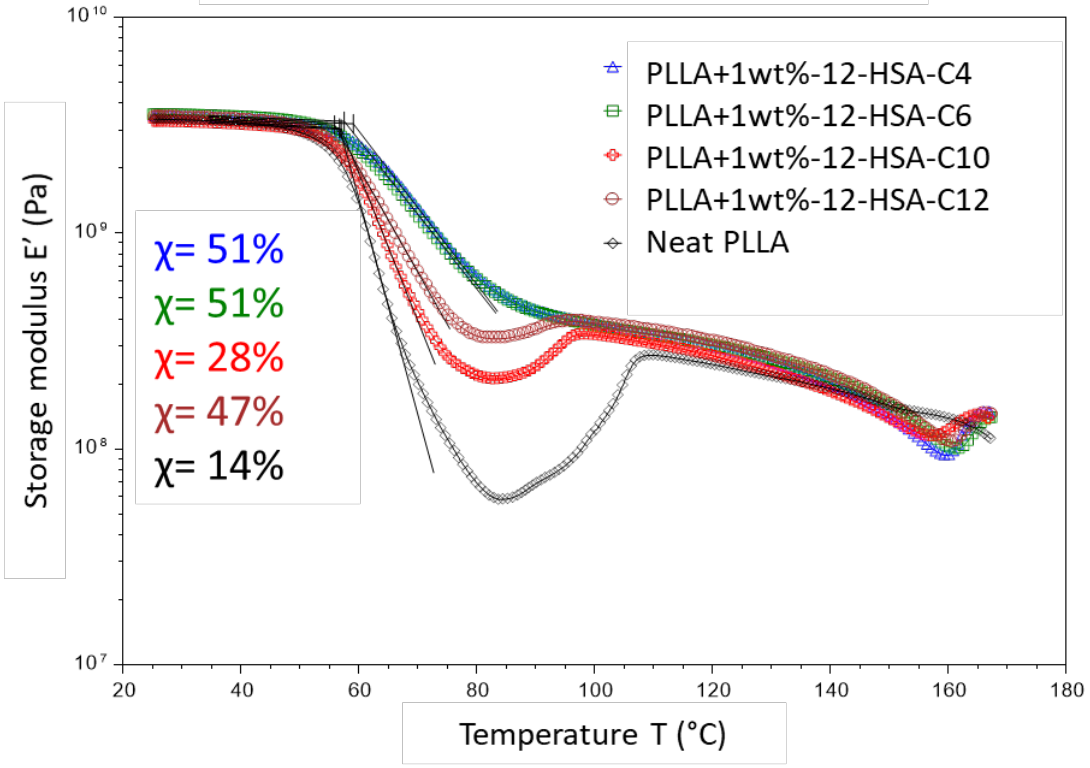

Figure 5. Storage modulus vs temperature (3°C/min (heating rate) for injection-moulded samples at 110°C for 1min 15s of PLLA mixed with 1wt% of: a) stearic acid derived bis-amides, b) 12-hydroxystearic derived bis-amides

*) Optimisation: Effect of time and loading

To further discriminate the nucleating agents, the composition of the samples was changed, namely, to diminish the amount of nucleating agent to see whether there would be an effect on the crystallisation performance. Here, the focus was narrowed to the most efficient nucleating agents which are the four ones made from the C4- and the C6-diamines with either stearic acid or 12-hydroxystearic acid. Three new loadings, 0.1wt%, 0.5wt and 0.8wt%, were tested, having already the data for a 1wt% loading. At the same time, a final optimisation was conducted by trying to reduce the moulding time, the lowest being 25s. The measured crystallinity ratios are displayed in Figure 6.

Figure 6

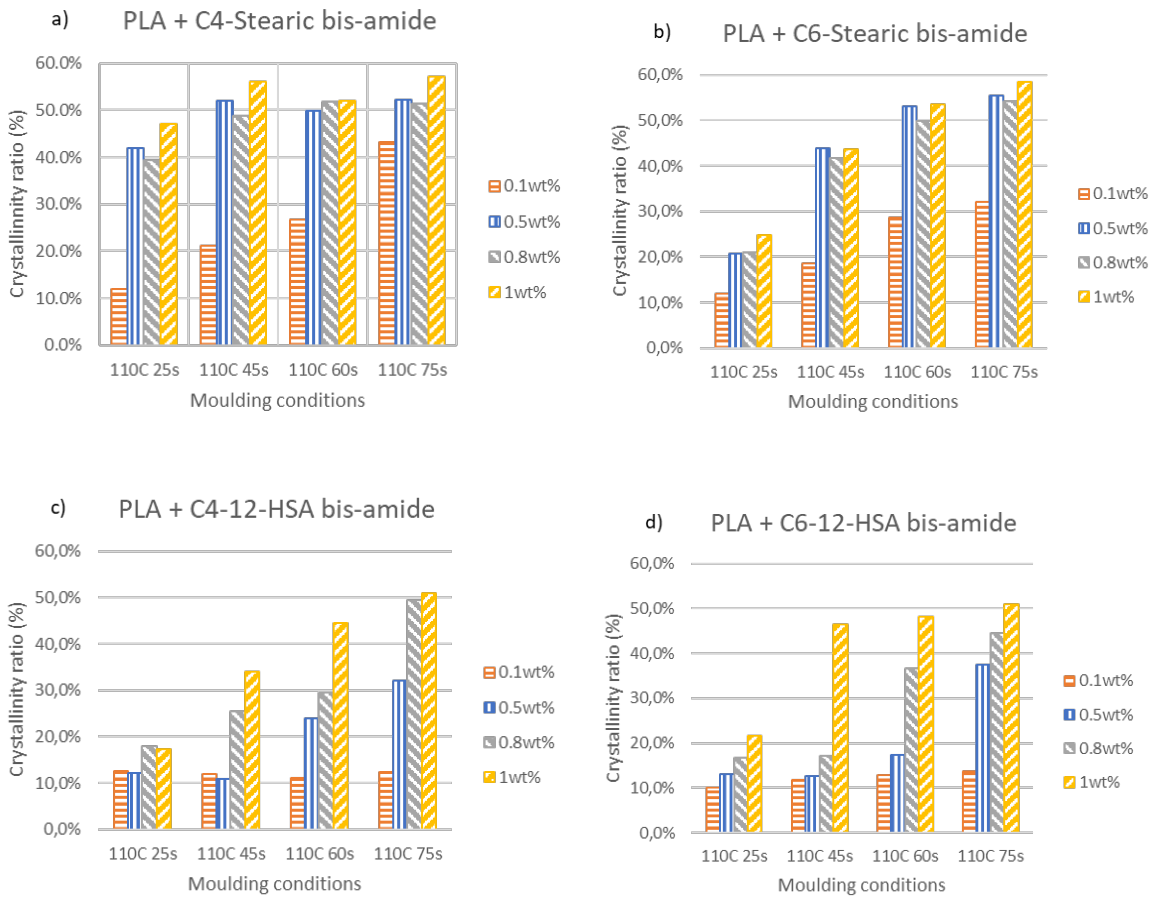

Figure 6. Crystallinity ratios in the DSC at 10°C/min (1st heating) for 4 moulding times at 110°C and 4 sample compositions with a) C4-stearic bis-amides, b) C6-stearic bis-amides, c) C4-12-HSA bis-amides, d) C6-12-HSA bis-amides

The C4-stearic bis-amide proves to be the best nucleating agent as reducing its amount had very little effect. Indeed, high degrees of crystallinity near or above 50% were still obtained at loadings from 0.5wt% and over. This was also observed when the moulding time was reduced, namely, going down to 45s, the crystallisation ratios were still nearing 50%. In the case of the shortest moulding time, 25s, there was a decrease in crystallinity ratio, this time averaging 40-45% depending on the loading. Three loadings achieved rather similar performances, meaning this

particular nucleating agent was indeed very efficient. In the case of a very small loading, 0.1wt%, a significant difference could be noticed in the crystallinity ratio. The crystallinity ratio still remained below 30% for moulding times up to 60s but went over 40% at 1min 15s also showing that the C4-stearic bis-amide nucleating agent is indeed very efficient in promoting the crystallisation of PLLA. Such performance was not achieved with the other considered nucleating agents.

The second-best performing nucleating agent is the other stearic acid derived bis-amide molecule. Crystallinity ratios near and over 50% were achieved for loadings from 0.5wt% to 1wt% but at moulding time of 1min and over. In the case of a 45s moulding time, the crystallisation ratio came down to 40% for these three loadings, again showing very little difference in behaviour between them. At the shortest moulding time however, the crystallinity ratio dropped to 20-25% for these three loadings, clearly indicating that such a short moulding time is insufficient using this nucleating agent.

Regarding the 12-HSA bis-amide samples, the latter achieved the lowest performances. At a 1wt% loading and long moulding times, high crystallinity ratios were obtained, however, they decreased rather quickly below 40% once the moulding time was shortened along with the loadings. Apart from the 1wt% loading, the crystallinity ratios also quickly fell below 25% when their amount was reduced, showing the need to use these NAs at high loadings and remain at 110°C for longer than the stearic based nucleating agents which were considered as the best nucleating agents.

Table 5

a) Fatty acid	Diamine	Weight ratio	HDT (°C)[a]	$\chi_{c,c}$ (%)[b]
Stearic	C4	0.1	**63**	**12**
		0.5	**104**	**42**
		0.8	**102**	**39**
		1	**111**	**47**
	C6	0.1	**62**	**12**
		0.5	**65**	**21**
		0.8	**66**	**21**
		1	**71**	**25**
12-hydroxystearic	C4	0.1	**62**	**13**
		0.5	**63**	**12**
		0.8	**63**	**18**
		1	**64**	**17**
	C6	0.1	**63**	**10**
		0.5	**64**	**13**
		0.8	**64**	**17**
		1	**64**	**22**

b) Fatty acid	Diamine	Weight ratio	HDT (°C)[a]	$\chi_{c,c}$ (%)[b]
Stearic	C4	0.1	**68**	**21**
		0.5	**111**	**52**
		0.8	**110**	**49**
		1	**109**	**56**
	C6	0.1	**64**	**19**
		0.5	**98**	**44**
		0.8	**101**	**42**
		1	**104**	**44**
12-hydroxystearic	C4	0.1	**63**	**12**
		0.5	**63**	**11**
		0.8	**71**	**25**
		1	**77**	**34**
	C6	0.1	**64**	**12**
		0.5	**68**	**13**
		0.8	**66**	**17**
		1	**104**	**47**

c) Fatty acid	Diamine	Weight ratio	HDT (°C)[a]	$\chi_{c,c}$ (%)[b]
Stearic	C4	0.1	**74**	**27**
		0.5	**114**	**50**
		0.8	**103**	**52**
		1	**123**	**52**
	C6	0.1	**71**	**29**
		0.5	**109**	**53**
		0.8	**106**	**50**
		1	**113**	**54**
12-hydroxystearic	C4	0.1	**64**	**11**
		0.5	**75**	**24**
		0.8	**78**	**29**
		1	**104**	**44**
	C6	0.1	**64**	**13**
		0.5	**69**	**17**
		0.8	**84**	**37**
		1	**99**	**48**

d) Fatty acid	Diamine	Weight ratio	HDT (°C)[a]	$\chi_{c,c}$ (%)[b]
Stearic	C4	0.1	**94**	**43**
		0.5	**112**	**52**
		0.8	**110**	**51**
		1	**119**	**57**
	C6	0.1	**76**	**32**
		0.5	**106**	**56**
		0.8	**108**	**54**
		1	**115**	**58**
12-hydroxystearic	C4	0.1	**66**	**12**
		0.5	**80**	**32**
		0.8	**96**	**49**
		1	**107**	**51**
	C6	0.1	**66**	**14**
		0.5	**87**	**38**
		0.8	**96**	**45**
		1	**105**	**51**

Table 5. HDTs and crystallinity ratios for samples moulded at 110°C for a) 25s, b) 45s, c) 60s & d) 75s

To further illustrate a direct consequence of a higher crystallinity ratio of PLLA samples, DMA measurements were also made along with the DSC analysis and the results are reported in Table 5. Here, the interest is to see the evolution of the storage modulus curve and more importantly whether a big loss after the Tg of PLLA could be noticed. This is reported through the HDT values, HDT values below 80°C accounting for a rather bad heat resistance of the sample. All the observations made previously are confirmed by the measured HDTs whose values reported in Table 5. Here again, as previously observed, the higher the crystallinity ratio, the higher the HDT. HDTs near or above 100°C could be achieved with crystallinity ratios approaching or above 40-45%, mainly with NAs derived from stearic acid. At short moulding times, e.g. 25s, only the samples made with C4-Stearic bis-amide at more than 0.5wt% loading exhibit high HDTs above 100°C along with crystallinity ratios above 40%. In the case of 12-hydroxystearic based bis-amides, HDT values above 100°C could only be achieved at high loadings (1wt%) and at moulding times over 1min, accounting for the lower performance of such nucleating agents.

The efficiency of the C4-Stear nucleating agent at very low loadings such as 0.1wt% is confirmed, since the HDT was significantly increased at moulding times of 1min15. Such performance could not be achieved with the other nucleating agents. Figure 7 is a typical illustration of the performance of the C4-stearic bis-amide nucleating agent regarding both the loading of the PLLA sample and the moulding time. First, the effect of different moulding times using a very low loading of nucleating agent, 0.1wt%, is displayed. The longer the sample stayed in the mould, the higher the crystallinity ratio but also the better its thermal behaviour as the fall of modulus becomes less and less appearing when the crystallinity ratio increases. In the best-case scenario, a rather smooth profile is obtained for the most crystalline sample. On the second plot, the effect of the amount of this particular nucleating agent in PLLA is shown. The shortest

moulding time (25s) was tested on purpose, hoping the achieved thermal performance would remain at its best. No PLLA reference is shown as samples could not be obtained in these processing conditions. As previously shown using DSC analysis, there is indeed very little difference between the highest loadings. Although the crystallinity ratios are slightly different (39% to 47%), the thermal behaviours are actually rather similar when looking at the graph. Logic is respected since a very small difference can be noticed as the more crystallised samples have slightly higher storage modulus values around 90°C. Such small difference emphasises the superior performance of the C4-Stear nucleating agent.

After the fall of modulus, two behaviours can be noticed, one regarding the 0.1wt% loaded samples and the other samples. The storage modulus for the 0.1wt% loaded samples increases strongly due to the cold crystallisation and the formation of α crystals and then reaches a plateau which lasts until the melting point of PLLA near 170°C. In the case of the other samples, this plateau does not exist, and the storage modulus continues to decrease until 160°C, then increases sharply and then starts to decrease again. This is due to the fact that the α' phase of PLLA has been preferentially formed for these samples. This phase has a lower melting point than the α phase, therefore explaining the decrease of storage modulus. The sharp increase at 160°C corresponds to the α' to α transition which results in more material remaining crystalline. Eventually, the storage modulus starts to drop around 170°C as the melting point of the α phase is reached.

Figure 7

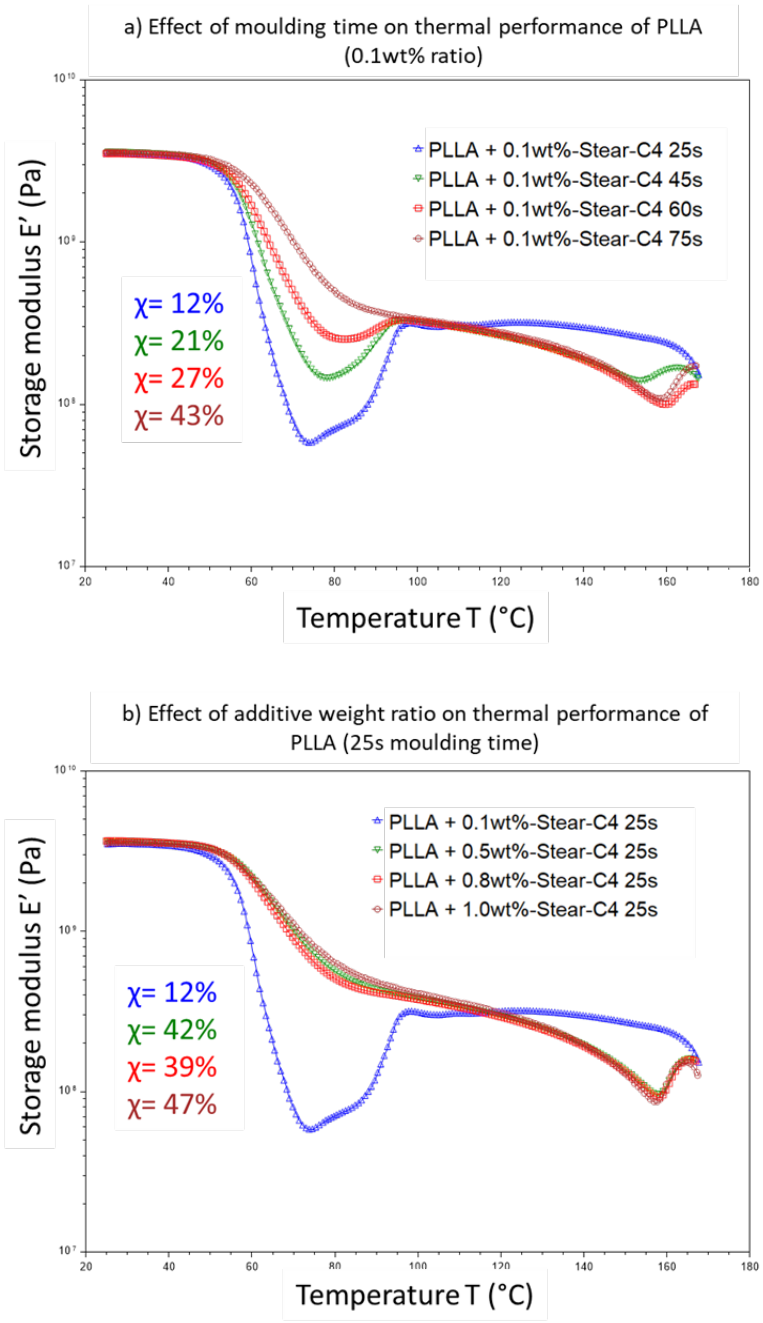

Figure 7. Storage modulus vs temperature of PLLA samples loaded with C4-stearic bis-amide. a) Effect of the moulding time on the thermal behaviour of the PLLA samples, b) Effect of the nucleating agent loading

CONCLUSION

In this part, we developed and used different nucleating agents derived from C18 fatty acids and linear aliphatic diamines. Using a thermal process, the corresponding bis-amide compounds were synthesised and through DSC analysis, discriminated the different compounds regarding their ability to enhance the crystallisation kinetics of PLLA.

The most efficient bis-amides are the ones obtained from stearic acid or 12-hydroxystearic acid using 1,4-diaminobutane or 1,6-diaminohexane *i.e.* compounds with short chain spacers, which displayed some of the highest melting points. In particular, the stearic acid based derivatives proved to have the highest melting points which resulted in the best performances with PLLA. More specifically, the C4-Stear bis-amide exhibited the best performance when mixed with PLLA. Using it, high crystallinity ratios over 50% were achieved along with the highest heat deflection temperatures nearing 120°C even at short moulding times. A clear effect of both the chain spacer and the fatty chain of the nucleating agent on the performance of the obtained material is demonstrated. However, this does not solve the brittleness problem of PLLA, therefore other additives should be considered. Other direct perspectives for this work would be to scale up the extrusion and the injection moulding process. Processing conditions should be optimised in order to obtain highly crystallised PLLA samples directly from the melt in industrial processing conditions.

ASSOCIATED CONTENT

Supporting Information. ^{1}H NMR spectra of all synthesised bis-amides, DSC traces of the bis-amides, WAXD patterns of PLLA samples loaded with 1wt% of all stearic acid derived nucleating agents and all 12-hydroxystearic acid-based compounds.

AUTHOR INFORMATION

Corresponding Author

* Henri Cramail – *Université de Bordeaux, CNRS, Bordeaux INP, LCPO, UMR 5629, F-33600 Pessac, France*

* Etienne Grau – *Université de Bordeaux, CNRS, Bordeaux INP, LCPO, UMR 5629, F-33600 Pessac, France*

Author Contributions

Jamie Rubinstein performed the experiments and data analysis and wrote the manuscript. Henri Cramail, Etienne Grau, Veronique Coma, Patrice Dole and Guillaume Chollet promoted the concept of the project.

Funding Sources

This work was financially supported by the Nouvelle-Aquitaine region, the ITERG and the CTCPA.

ACKNOWLEDGMENT

The authors want to thank the ITERG and the CTCPA for their involvement in this research work. Along with them, the LCPO technical staff and personnel are deeply thanked for their help with the experiments and the characterisations.

REFERENCES

(1) European Bioplastics.

(2) *Polylactic Acid (PLA) Market | 2022 - 2026 | MarketsandMarkets*. https://www.marketsandmarkets.com/Market-Reports/polylactic-acid-pla-market-29418964.html (accessed 2022-06-01).

(3) Kalb, B.; Pennings, A. J. General Crystallization Behaviour of Poly(l-Lactic Acid). *Polymer* **1980**, *21* (6), 607–612. https://doi.org/10.1016/0032-3861(80)90315-8.

(4) Miyata, T.; Masuko, T. Crystallization Behaviour of Poly(l-Lactide). *Polymer* **1998**, *39* (22), 5515–5521. https://doi.org/10.1016/S0032-3861(97)10203-8.

(5) Saeidlou, S.; Huneault, M. A.; Li, H.; Park, C. B. Poly(Lactic Acid) Crystallization. *Prog. Polym. Sci.* **2012**, *37* (12), 1657–1677. https://doi.org/10.1016/j.progpolymsci.2012.07.005.

(6) Nam, J. Y.; Okamoto, M.; Okamoto, H.; Nakano, M.; Usuki, A.; Matsuda, M. Morphology and Crystallization Kinetics in a Mixture of Low-Molecular Weight Aliphatic Amide and Polylactide. *Polymer* **2006**, *47* (4), 1340–1347. https://doi.org/10.1016/j.polymer.2005.12.066.

(7) Xing, Q.; Zhang, X.; Dong, X.; Liu, G.; Wang, D. Low-Molecular Weight Aliphatic Amides as Nucleating Agents for Poly (L-Lactic Acid): Conformation Variation Induced Crystallization Enhancement. *Polymer* **2012**, *53* (11), 2306–2314. https://doi.org/10.1016/j.polymer.2012.03.034.

(8) Xing, Q.; Li, R.; Zhang, X.; Dong, X.; Wang, D.; Zhang, L. Tailoring Crystallization Behavior of Poly (l-Lactide) with a Low Molecular Weight Aliphatic Amide. *Colloid Polym. Sci.* **2015**, *293* (12), 3573–3583. https://doi.org/10.1007/s00396-015-3730-5.

(9) Chen, L.; Dou, Q. Influence of the Combination of Nucleating Agent and Plasticizer on the Non-Isothermal Crystallization Kinetics and Activation Energies of Poly(Lactic Acid). *J. Therm. Anal. Calorim.* **2020**, *139* (2), 1069–1090. https://doi.org/10.1007/s10973-019-08507-y.

(10) Saitou, K.; Yamaguchi, M. Transparent Poly(Lactic Acid) Film Crystallized by Annealing beyond Glass Transition Temperature. *J. Polym. Res.* **2020**, *27* (4), 104. https://doi.org/10.1007/s10965-020-02071-y.

(11) Takenaka, A.; 武中晃; Nomoto, S.; 野本昌吾; Matsuo, T.; 松尾俊樹; Kimura, H.; 木村栄紀. Manufacturing Method of Biodegradable Resin Molding. JP2007130895A, May 31, 2007.

(12) Onishi, H.; Morishita, K. Polylactic Acid Resin Composition and Resin Molded Article Thereof. US9376546B2, June 28, 2016.

(13) Fischer, E. W.; Sterzel, H. J.; Wegner, G. Investigation of the Structure of Solution Grown Crystals of Lactide Copolymers by Means of Chemical Reactions. *Kolloid-Z. Z. Für Polym.* **1973**, *251* (11), 980–990. https://doi.org/10.1007/BF01498927.

(14) Sato, K. Crystallization Behaviour of Fats and Lipids — a Review. *Chem. Eng. Sci.* **2001**, *56* (7), 2255–2265. https://doi.org/10.1016/S0009-2509(00)00458-9.

(15) Himawan, C.; Starov, V. M.; Stapley, A. G. F. Thermodynamic and Kinetic Aspects of Fat Crystallization. *Adv. Colloid Interface Sci.* **2006**, *122* (1–3), 3–33. https://doi.org/10.1016/j.cis.2006.06.016.

(16) Poopalam, K. D.; Raghunanan, L.; Bouzidi, L.; Yeong, S. K.; Narine, S. S. The Anomalous Behaviour of Aliphatic Fatty Diamides: Chain Length and Hydrogen Bonding Interactions. *Sol. Energy Mater. Sol. Cells* **2019**, *201*, 110056. https://doi.org/10.1016/j.solmat.2019.110056.

(17) Stempfle, F.; Ortmann, P.; Mecking, S. Long-Chain Aliphatic Polymers To Bridge the Gap between Semicrystalline Polyolefins and Traditional Polycondensates. *Chem. Rev.* **2016**, *116* (7), 4597–4641. https://doi.org/10.1021/acs.chemrev.5b00705.

(18) Vasanthakumari, R.; Pennings, A. J. Crystallization Kinetics of Poly(l-Lactic Acid). *Polymer* **1983**, *24* (2), 175–178. https://doi.org/10.1016/0032-3861(83)90129-5.

(19) De Santis, F.; Pantani, R.; Titomanlio, G. Nucleation and Crystallization Kinetics of Poly(Lactic Acid). *Thermochim. Acta* **2011**, *522* (1–2), 128–134. https://doi.org/10.1016/j.tca.2011.05.034.